X-ray/optical observations of stars with shallow convection zones (A8−G2 V)⋆

A.J.M. Piters[1], J. van Paradijs[1,2], and J.H.M.M. Schmitt[3]

[1] Astronomical Institute "Anton Pannekoek" / CHEAF, Kruislaan 403, NL-1098 SJ Amsterdam, The Netherlands
[2] Physics Department UAH, Huntsville, AL 35899, U.S.A.
[3] Max Planck Institut für Extraterrestrische Physik, Giessenbachstraße 1, 8046 Garching bei München, Germany

Abstract. We present Walraven photometry and ROSAT All-Sky Survey data for a sample of 173 bright main-sequence stars with spectral types between A8V and G2V. These observations are part of a study of the onset of magnetic surface activity along the main sequence. Values for the effective temperature, surface gravity and interstellar reddening have been obtained from a comparison of the observed Walraven colours with theoretical values. These parameters have been used to derive accurate X-ray surface flux densities.

Key words: stars: activity; fundamental parameters — X-rays: stars

1. Introduction

Stars with spectral types later than ∼F5 show magnetic surface activity, chromospheres and coronae like the Sun. Stars with earlier spectral types appear to have a weaker outer atmosphere, supposedly due to the shallowness or absence of outer convection zones in these stars (Schrijver 1993, and references therein). As part of a study of the onset of stellar activity along the main sequence, we have used ROSAT all-sky survey data to determine X-ray fluxes of a sample of 173 main-sequence stars, with spectral types between A8 and G2. In order to derive detailed quantitative information on the location of these stars in the Hertzsprung-Russell diagram, we have also made Walraven five-colour photometric observations.

The sample studied here was selected from the Bright Star Catalogue (BSC; Hoffleit & Jaschek 1982, lists almost

⋆ Tables 1, 2 and 5 are only available in electronic form at the CDS via anonymous ftp to cdsarc.u-strasbg.fr (130.79.128.5) or via http://cdsweb.u-strasbg.fr/Abstract.html

all stars with $V_{\rm J} < 6.5$ mag) according to the following criteria:

– Spectral type between A8 and G2; no spectral peculiarities noted; not double in spectral type classification (e.g., HR 32 with spectral type F2V+F6V is excluded).
– Luminosity class V;
– Right ascension between $0^{\rm h}$ and $2^{\rm h}$, or between $14^{\rm h}$ and $24^{\rm h}$, declination south of $+10°$ (defining the region on the sky visible during the appointed observation times);
– Binaries for which both components occurred in the BSC are excluded, if the separation is less than $10''$.

The selected sample is listed in Table 1, excluding five stars for which no (photometric and X-ray) data are available (HR 591, HR 5542, HR 6593, HR 8245, HR 8735). Four stars have not been observed in the Walraven photometric system, and for 11 stars we have no ROSAT data available. These 15 stars with incomplete data are indicated as such in Table 1.

This paper reports the results of the ROSAT and Walraven observations. Spectroscopic observations and determinations of the rotational velocities for the sample stars have been described in Groot et al. (1996).

2. Walraven photometry

2.1. The observations

The photometric observations were made during 11 nights in 1989 between June 21 and July 29, with the Walraven photometer on the 90 cm Dutch telescope at the European Southern Observatory. This photometer (Lub & Pel 1977) provided simultaneous measurements of the stellar brightness in five passbands (called V, B, U, W, and L), between 3250 and 5500 Å. All measurements were made using a diaphragm with a 16 arcsecond diameter. An observation of each star consisted of four integrations of 16 seconds each, followed by two such integrations on the

Table 3. The correction factor $f(n)$ to the uncertainty in the mean value and the correction factor $g(n)$ to the standard deviation for a small number of observations n

n	$f(n)$	$g(n)$	n	$f(n)$	$g(n)$	n	$f(n)$	$g(n)$
2	1.84	1.49	6	1.11	1.07	10	1.06	1.04
3	1.32	1.20	7	1.09	1.06	11	1.05	1.03
4	1.20	1.13	8	1.08	1.05	12	1.05	1.03
5	1.14	1.09	9	1.07	1.04			

Table 4. The average standard deviations of the observations with their spread

$\overline{\sigma}_{V_{\mathrm{W}}}$	0.0028 ± 0.0018
$\overline{\sigma}_{(V-B)_{\mathrm{W}}}$	0.0015 ± 0.0008
$\overline{\sigma}_{(B-U)_{\mathrm{W}}}$	0.0016 ± 0.0008
$\overline{\sigma}_{(U-W)_{\mathrm{W}}}$	0.0026 ± 0.0013
$\overline{\sigma}_{(B-L)_{\mathrm{W}}}$	0.0016 ± 0.0008

sky background. Most stars were observed during more than one night. The number of observations for each star (ranging from 1 to 7, with one exception of 12 observations) are listed in Table 2.

The observations were tied to the Walraven photometric system by measurements of (typically 7) standard stars at the beginning, middle and end of each night.

The visual brightness (V_{W}) and colour indices (($V-B)_{\mathrm{W}}$, $(B-U)_{\mathrm{W}}$, $(U-W)_{\mathrm{W}}$ and $(B-L)_{\mathrm{W}}$) of the programme stars were obtained, using linear fits to the standard-star observations, as a function of $\sec z$ (z is the zenith distance):

$$V_{\mathrm{W}} = \log S_V - k_V \sec z + Q_V \qquad (1)$$
$$(V-B)_{\mathrm{W}} = \log(S_V/S_B) - k_{VB} \sec z + Q_{VB}, \qquad (2)$$

where S_V and Q_V are the (sky-corrected) signal and zero point in the V channel, respectively. Similar expressions were used for the other colour indices. (As is customary in the Walraven system, the brightness and colours of a star are given on a $\log_{10}$ scale, and not in magnitudes.)

The Walraven V and colours obtained for each star during different nights, have been averaged. The uncertainties in the mean values, as listed in Table 2, have been estimated as follows. The square root of the sample variance, $s \equiv \sqrt{\sum(x_i - \overline{x})^2/(n-1)}$, is not a good estimate of the standard deviation for small numbers of observations, and $\Delta \overline{x} = s/\sqrt{n}$ (n being the number of observations), is not a good estimate of the error in the mean value (Burington & May 1970). We have estimated a correction factor $f(n)$ to the error $\Delta \overline{x}$ in the mean value $\overline{x}$ and a correction factor $g(n)$ to the standard deviation s, as a function of the number of measurements using a computer simulation. From a normal distribution with mean μ and standard deviation σ we have drawn 10^6 times n random numbers, each time calculating the sample standard deviation s and the sample mean value $\overline{x}$. The 10^6 standard deviations found in this way for each n are averaged. The correction factor $g(n)$ is the standard deviation of the parent population divided by the average sample standard deviation derived from the simulation. The correction factor $f(n)$ is the standard deviation of the 10^6 values for $(\overline{x}-\mu)/(s/\sqrt{n})$. The correction factors are listed in Table 3. The uncertainties in the Walraven brightness and

colours have been estimated using the corrected formula $\Delta \overline{x} = f(n)s/\sqrt{n}$.

If an observation deviated from the corresponding mean value by more than four times the standard deviation (derived from the other observations of the same source) for all colours, it was excluded from the analysis. Only two observations were excluded in this way.

A measure of the accuracy of the photometry is given by the standard deviation of consecutive observations of the brightness and colours of each star, provided that the star is not intrinsically variable. Table 4 lists the average standard deviations $\overline{\sigma}$ (corrected for small n as described above) of the brightness and colours and their spread $s_{\overline{\sigma}}$. In the present sample, it is found that the average standard deviation does not depend on brightness. In calculating this average, we left out 12 stars which appeared to be variable in brightness or in one or more colours, having standard deviations significantly larger (more than $4s_{\overline{\sigma}}$) than the average standard deviation. These stars are indicated in Table 2 with an asterisk. The average standard deviation and its spread was used to assign uncertainties to the brightness and colours of stars, that were only measured once. These uncertainties, as listed in Table 2, were taken equal to $\overline{\sigma} + 3s_{\overline{\sigma}}$ (from Table 4).

A diagram of $(B-U)_{\mathrm{W}}$ against $(V-B)_{\mathrm{W}}$ is shown in Fig. 1. All stars, but five, lie in a narrow band with a width of about 0.06 in log (flux) (≈ 0.15 mag). The three sources that lie above this band are: HR 6843, HR 8646 and HR 8917. The deviation of these three stars could be caused by large interstellar or circumstellar reddening (the spectral classification of these stars also predicts a much smaller colour index than observed). The two stars that lie below this band are HR 5356 and HR 8181.

2.2. Comparison with Johnson's photometric system

The difference between the Walraven apparent brightness V_{W} and the apparent brightness obtained from Johnson's apparent visual magnitude V_{J} appears to depend slightly on colour $(V-B)_{\mathrm{W}}$. Johnson's apparent visual magnitudes have been obtained from the Bright Star Catalogue (BSC) (Hoffleit & Jaschek 1982). For the stars in our sample,
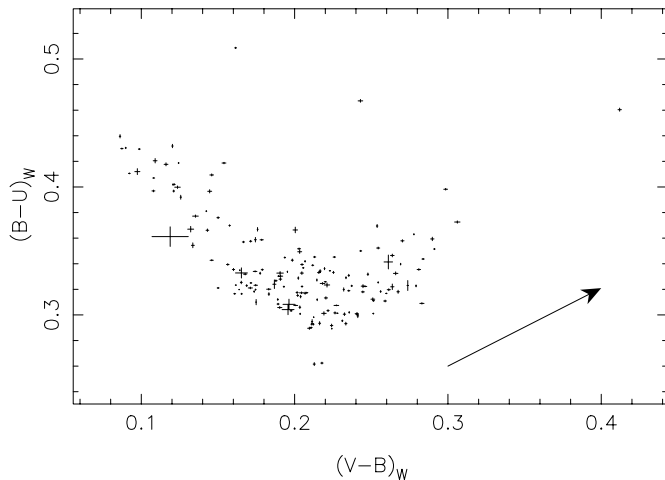
Fig. 1. Colour-colour diagram of the Walraven colours $(B-U)_W$ and $(V-B)_W$. The error bars indicate the uncertainties in the colours as listed in Table 2, the arrow indicates an interstellar reddening of 0.1 dex in $(V-B)_W$
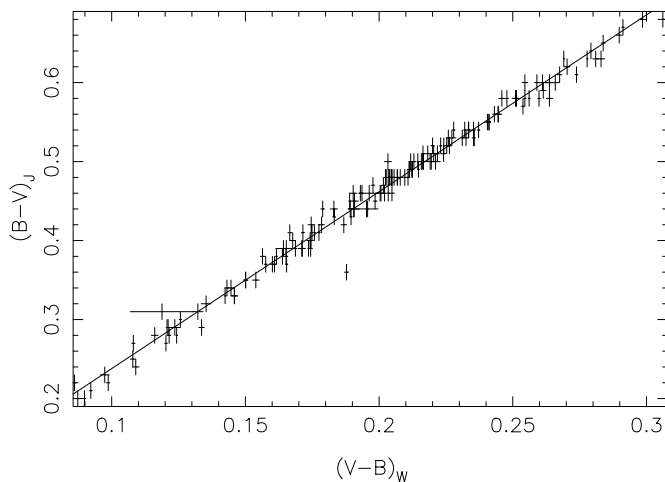

Fig. 2. A comparison of Johnson's $(B-V)_J$ with the Walraven colour $(V-B)_W$. The error bars indicate the uncertainties in the colours, as listed in Table 2. For $(B-V)_J$ an uncertainty of 0.01 is assumed. The solid line is given by Eq. (4)

excluding the five deviating stars from Sect. 2.1, the best-fit linear relation is given by:

$$V_J = -0.11(\pm 0.06)(V-B)_W - 2.5[V_W - 2.747(\pm 0.005)] . \quad (3)$$

The Walraven $(V-B)_W$ colour and Johnson's $(B-V)_J$ are tightly related (Fig. 2). The best linear fit for our sample (excluding the five deviating stars from Sect. 2.1) is given by:

$$(B-V)_J = 0.014(\pm 0.004) + 2.239(\pm 0.017)(V-B)_W . \quad (4)$$

The relations 3 and 4 are consistent with those derived by Van Paradijs et al. (1986) for a sample of OB-type stars.
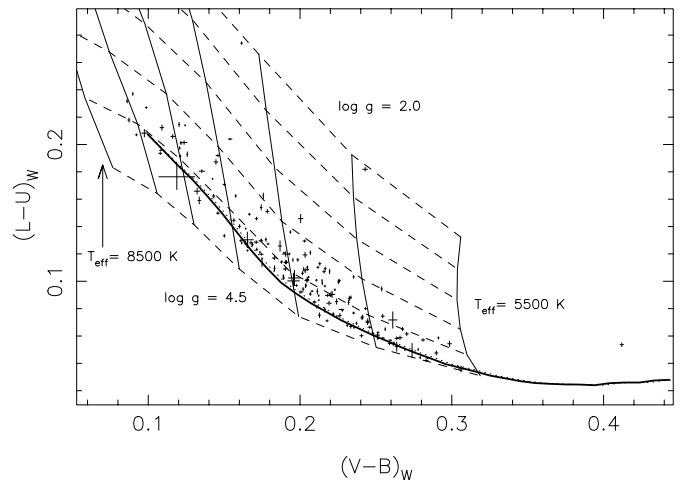

Fig. 3. Colour-colour diagram of $(V-B)_W$ vs. $(L-U)_W$. Lines of equal surface gravity $\log g$ (in steps of $\Delta \log g = 0.5$; dashed lines) and equal effective temperature T_{eff} (in steps of $\Delta T = 500$ K; solid lines) are from corrected colours of Kurucz models, calibrated with Hyades main-sequence stars (see text). The Hyades main-sequence ([Fe/H] = 0.12) is plotted as a dotted line, and the adopted main-sequence for solar abundance as a thick solid line. Crosses denote the location of our sample stars, the error bars indicate the uncertainties as listed in Table 2

One star, HR 7126 with $(B-V)_J = 0.36$ and $(V-B)_W = 0.1878$, has a large deviation from this relationship, which is probably due to an error in the BSC value for $(B-V)_J$. For instance, the Hipparcos input catalogue (Turon et al. 1992), lists for this star $(B-V)_J = 0.44$, which puts it right on the relationship defined by Eq. (4).

3. Stellar parameters

The effective temperature T_{eff}, surface gravity g, and interstellar extinction $E(V-B)$ (in the Walraven system) were derived for each star from a comparison of the observed Walraven colours with theoretical values. The theoretical $(V-B)_W$ and $(L-U)_W$ values as functions of T_{eff} and $\log g$ were obtained from an empirically derived main-sequence relation between T_{eff}, $\log g$, $(V-B)_W$ and $(L-U)_W = (B-U)_W - (B-L)_W$ for the Hyades, combined with differential colour-colour vectors from a folding of the Walraven passbands with the spectral energy distributions for a grid of Kurucz (1992) model atmospheres. Both the empirical Hyades main-sequence and the differential vectors for the Kurucz model atmospheres were kindly provided by Pel (1991). The models used cover the effective temperature range from 5500 K to 8500 K and the surface gravity range 2.0 to 4.5. Chemical abundances range from 0.003 times the solar value to the solar value. We have converted the empirically derived Hyades main-sequence relation, with [Fe/H] = 0.12, to a relation valid for solar abundances, and extrapolated it

to lower surface gravity values, using differential vectors from Kurucz model atmospheres. The use of differential vectors bypasses possible systematic offsets in the colours derived from Kurucz model atmospheres. Figure 3 shows the resulting $(V-B)_W - (L-U)_W$ diagram with lines of constant temperature and surface gravity, for solar abundances. Also, the location of the empirical Hyades main-sequence is indicated (dotted line, [Fe/H] = 0.12) and the main sequence as converted to solar abundance (thick solid line), and the positions of the sample stars are plotted. For a subsample of stars with supposedly small interstellar reddening, preliminary values for the effective temperature and the surface gravity were derived by equating the observed $(V-B)_W$ and $(L-U)_W$ with the theoretical ones. The subsample was checked for consistency on the assumed interstellar reddening, after deriving the extinction for every star by comparing with the (corrected) theoretical Walraven colours. These preliminary values for the effective temperature and the surface gravity were used to calculate the expected theoretical colours $(B-U)_W$ and $(U-W)_W$ for the same subsample. The differences between observed and theoretical values were interpreted as a systematic error in the theoretical colours, and were used to correct the theoretical colours. The colour $(B-L)$ is corrected using the corrections for $(B-U)$ and $(L-U)$.

After that, values for T_{eff}, $\log g$ and $E(V-B)$ were derived by comparing their observed colours $((V-B)_W$, $(B-U)_W$, $(B-L)_W$, $(U-W)_W)$ with the corrected theoretical ones. If any of the stars, used for calibration, had significant extinction the whole procedure was repeated, without these reddened stars.

The final values for T_{eff}, $\log g$ and $E(V-B)$ for all stars, as listed in Table 2, their uncertainties and the uncertainties $\sigma^2_{i,\text{th}}$ on the theoretical colours $C_{i,\text{th}}$, have been derived simultaneously by minimising χ^2:

$$\chi^2 = \sum_{i=1}^{4} \frac{(C_{i,\text{obs}} - C_{i,\text{th}})^2}{\sigma^2_{i,\text{obs}} + \sigma^2_{\text{th}}}, \qquad (5)$$

where $C_{i,\text{obs}}$ and $\sigma_{i,\text{obs}}$ are the observed colour and its uncertainty, respectively. The uncertainties on the stellar parameters are determined by the values where χ^2 equals the minimum χ^2 plus one, and the uncertainties in the theoretical colours are determined by assuming that the quadratic deviation between the observed and the theoretical colour $C_{i,\text{obs}} - C_{i,\text{th}}$ is on average equal to the sum of their quadratic uncertainties $\sigma^2_{i,\text{obs}} + \sigma^2_{\text{th}}$.

We find that for the present sample the uncertainties in the theoretical colours are negligible in $(V-B)_W$ and $(B-U)_W$ (compared to the observational uncertainties). The uncertainty in the theoretical $(U-W)_W$ is 0.013, and the uncertainty in the theoretical $(B-L)_W$ is 0.015.

The uncertainties in the effective temperature, the surface gravity, and the colour excess $E(V-B)$, are typically (68%): 60 K < ΔT_{eff} < 170 K, 0.05 < $\Delta \log g$ < 0.17, and

$0.004 < \Delta E(V-B) < 0.009$, respectively. An extra (unknown) uncertainty may occur if the stellar parameters are outside the range of the parameters of the calibration stars (T_{eff} between 6000 K and 8000 K; $\log g$ between 3.4 and 4.4).

For five stars (HR 313, HR 7126, HR 8041, HR 8917 and HR 8935) we could not find consistent stellar parameters with this method, in the sense that the minimum χ^2 for these stars is larger than 10. We can find no reason why these stars should deviate in their colour-colour behaviour. These stars are indicated in Table 2 with a colon after the values. No uncertainties are given for these stars.

4. The X-ray data

The ROSAT All-Sky Survey was conducted from July 1990 until January 1991. During the survey the satellite scanned the sky in circles perpendicular to the direction of the Sun. Any particular position in the sky was in the 2° field of view of the Position Sensitive Proportional Counter (PSPC) for about 30 seconds once every 90 minutes, during at least 2 days (depending on the ecliptic latitude). The PSPC is sensitive in the energy range 0.1−2.4 keV. For a detailed description of the satellite and the PSPC we refer to Trümper (1983) and Pfeffermann et al. (1988), and for a description of the All-Sky Survey to Voges (1992).

The X-ray count rates have been derived as described in Chapter 2 of Piters (1995). A short summary will be given here. We selected a region around the position of the source, and two background regions on the same ecliptic longitude (i.e. on the same survey scans). From the number of counts in these three regions, and their effective exposure times we derived the most probable source count rate and its uncertainty, using a maximum-likelihood method based on Poisson statistics. A 3σ upper limit to the count rate is determined if the probability P_{bg} that the counts in the source region are only background counts is larger than 0.025. With this threshold value we expect only 0.5 false detections in our sample (determined by the sum of P_{bg} over all detections).

The resulting count rates and upper limit values are given in Table 5 (Col. 2). We detected 86 X-ray sources out of the total of 162 stars for which X-ray data were available.

The conversion of count rate r_s to flux density (ergs cm^{-2}s^{-1}) at Earth f_X is given by

$$f_X = \frac{r_s}{C_X} \qquad (6)$$

where C_X is the energy-conversion factor, derived from the hydrogen column density n_H, and from the probability distribution of the hardness ratio $q(h)$, following the procedure as described in Chapter 2 of Piters (1995). This method assumes that the X-ray spectrum can be described by a single-temperature Mewe & Gronenschild

(Mewe et al. 1985) spectrum which is subject to galactic absorption (Morrison & McCammon 1983). From the probability distribution of the hardness ratio (defined as the ratio of the source count rate in the high-energy band — channels 41 to 240, $\sim 0.4 - 2.4$ keV — and the total source count rate) we derive a probability distribution for the temperature. Because every temperature is associated with a value for C_X the most probable value for C_X and its uncertainty interval can be calculated from this distribution of temperature. The most probable value for the hardness ratio and its uncertainty are listed in Col. 3 of Table 5, and the most probable value for C_X and its uncertainty interval are listed in Col. 4 of Table 5. For nearby stars in the galactic plane (distance less than 200 pc and galactic latitude between $-30°$ and $+30°$) we derived n_H from Paresce (1984), while for more distant stars we estimated n_H from the interstellar reddening $E(V - B)$, as derived in Sect. 3, using the relation $E(B - V) = 2.39E(V - B) - 0.17E(V - B)^2$ and the expression $n_H = 5.8 \ 10^{21}E(B - V)\mathrm{cm}^{-2}$ (Bohlin et al. 1978; close to the relation recently derived by Predehl & Schmitt 1995). The spread around this relationship is about 30%. The distance is derived from the parallax or, if the parallax is not known, from the distance modulus. The adopted n_H values are listed in Table 5, Col. 5.

For each star detected in the ROSAT survey we derived the X-ray flux density at the stellar surface, F_X, the X-ray luminosity L_X, and the normalised X-ray flux density $R_X = L_X/L_{bol}$ from the flux density at the detector, f_X:

$$\log R_X = \log f_X + 0.4(V_J + BC) + 4.574, \qquad (7)$$

$$\log F_X = \log R_X + 4\log T_{eff} - 4.246, \qquad (8)$$

$$\log L_X = \log F_X + 2\log(R_*/R_\odot) + 22.784. \qquad (9)$$

The effective temperatures T_{eff} have been taken from Table 2, the bolometric correction BC from Hayes (1978), who gives these corrections as a function of the effective temperature. Johnson's apparent visual magnitudes V_J have been obtained from the extinction corrected Walraven brightness V_W and colour $(V - B)_W$ using Eq. (3). The stellar radii R_* have been derived from the surface gravity, using the relation $R_* = \sqrt{GM/g}$. The mass M is calculated as a function of effective temperature from the mass-spectral type relation, as given by Schmidt-Kaler (1982), combined with the spectral type-temperature relation as given by Hayes (1978). The numerical constants are based on the solar parameters used by Oranje et al. (1982). The values for $\log F_X$, $\log L_X$ and $\log R_X$ and their uncertainties are listed in Table 5, Cols. 6

to 8. These uncertainties are dominated by the uncertainties in the source count rate r_s and in the hydrogen column density n_H, the latter being caused by the relatively large uncertainties in the distance and in $E(V - B)$.

References

Bohlin R.C., Savage B.D., Drake J.F., 1978, ApJ 224, 132

Burington R.S., May D.C., 1970, Handbook of probability and statistics with tables, 2nd edition. McGraw-Hill, New York-London

Groot P.J., Piters A.J.M., Van Paradijs J., 1996 (accepted by A&A)

Hayes D.S., 1978, IAU Symp. 80, p. 65

Hoffleit D., Jaschek C., 1982, The Bright Star Catalogue, 4th Rev. ed. Yale University Observatory, New Haven CT

Kurucz R.L., 1992, in Barbuy B., Renzini A. (eds.), IAU Symp. 149, "The Stellar Populations of Galaxies". Dordrecht, Kluwer, p. 225

Lub J., Pel J.W., 1977, A&A 54, 137

Mewe R., Gronenschild E.H.B.M., Van den Oord G.H.J., 1985, A&A 62, 179

Morrison R., McCammon D., 1983, ApJ 270, 119

Oranje B.J., Zwaan C., Middelkoop F., 1982, A&A 110, 30

Paresce, 1984, AJ 89, 1022

Pel J.W. (private communication)

Pfeffermann E., Briel U.G., Hippmann H., et al., 1988, Proc. SPIE 733, 519

Piters A.J.M., 1995, Ph.D. thesis, University of Amsterdam

Predehl P., Schmitt J.H.M.M., 1995, A&A 293, 889

Schmidt-Kaler Th., 1982, in: Scaifers K., Voigt H.H. (eds.), Landolt-Börnstein: Numerical Data and Functional Relationships in Science and Technology. Springer-Verlag, Berlin. Vol. 2b, p. 453

Schrijver C.J., 1993, A&A 269, 446

Trümper J., 1983, Adv. Space Res. 2, 241

Turon C., et al., 1992, The Hipparcos Input Catalogue, ESA SP-1136

Van Paradijs J., Van Amerongen S., Damen E., Van der Woerd H., 1986, A&AS 63, 71

Voges W., 1992, ESA ISY-3, p. 9